Available online at www.sciencedirect.com

ScienceDirect

IFAC PapersOnLine 58-15 (2024) 426–431

# A practical approach for transfer function estimation using short, transient process data ⋆

**Robin De Keyser** * **Isabela R. Birs** *, ** **Cristina I. Muresan** ** **Clara M. Ionescu** *, **

* *Department of Electromechanical, Systems and Metal Engineering Flanders Make EEDT Core lab, Ghent University, Tech Lane Science Park 125 and 131, 9052, Gent, Belgium (e-mail: Claramihaela.Ionescu@ugent.be, Robain.DeKeyser@ugent.be).*

** *Department of Automation Technical University of Cluj Napoca, Memorandumului nr 28, 400114 Cluj-Napoca, Romania (e-mail: Cristina.Muresan@aut.utcluj.ro, Isabela.Birs@aut.utcluj.ro)*

**Abstract:**
Increased productivity in the industrial sector requires optimal closed loop performance. This can be solely achieved through optimal tuning of the controller parameters, which requires reliable and efficient process data, further employed in process estimations or high quality models. Most of the classical identification methods require long input-output data sets. In this paper we propose a technique to extract process information from short transient process data. The method is based on short sine test which can be superimposed on nominal process inputs, and estimates the process impulse response, consequently providing a band limited, but highly accurate, frequency response. This in turn is used to accurately estimate a high order plus dead time model. The method is reliable and requires less effort compared to classical step based methods. The main features of the proposed method are: 1) it uses a short duration test based on a sine input; 2) it produces accurate models in the presence of stochastic disturbances; and 3) it can be executed in open or closed loop. Numerical examples are provided to validate the theoretical approach and demonstrate the accuracy of the estimation.



*Keywords:* closed loop frequency domain identification, transient process data, robustness

## 1. INTRODUCTION

Industry is widely dominated by the Proportional-Integrative-Derivative (PID) controller (Åström and Hägglund (2004)) due to its simplicity and ease of implementation. Most of the times, these PIDs are not meeting optimal criteria, due to poor tuning. To optimally tune these controllers, a process model or significant information on the process is required. Sometimes obtaining such information implies interfering with the process while it is operating. To minimise losses, gathering process data fast is of paramount importance. This data can later on be used to estimate a transfer function for the process, which can be in turn used in the retuning of the PID controller parameters.

Open loop or closed loop tests can be used to extract relevant process data. In (Ziegler and Nichols (1942)), closed loop tests are designed in order to obtain process information. These were later replaced by relay methods (Åström and Hägglund (1984)) in various approaches (K.K. Tan and Wang (1996)), (Monje et al. (2008)). They were used to estimate the process frequency response, at various frequencies, usually the critical one. Step response data, either obtained using open or closed loop tests (Jianhong and Ramirez-Mendoza (2020)), was also used to estimate simple models, such as second order plus dead time (De Keyser and Muresan (2019)), (Muresan et al. (2023)). Impulse response data were also used as a means to estimate process transfer functions (Xu and Ding (2017)), (Xu et al. (2021)), (Xu and Yang (2020)). These are just a few of the plethora of transfer function estimation methods available and reported in literature. Excellent review papers on these estimation methods can be found in (Albertos (2014)), (Liu et al. (2013)) or (Ljung et al. (2020)), to name just a few. Although reliable, these methods are characterised by the large amount of data needed to estimate the process transfer function. This is a major disadvantage for the industrial sector when shutting down the plant to collect data ultimately leads to low productivity and profit.

This paper presents a new simple and reliable methodology to extract relevant process data with an immediate practical applicability regarding transfer function estimation. The main features are: 1) short transient data is required (not steady state data as with other existing methods); 2) accurate estimation in the presence of stochastic disturbances; 3) works for both open and closed loop data. The methodology consists of simple steps: i) a sinusoidal signal of a desired test frequency is constructed; ii) the sinusoidal signal is applied to the process and the corresponding output is measured and recorded. Next, the impulse response is determined and used to accurately estimate the frequency response of the process at some specific frequencies around the test frequency. One can now determine an accurate high order plus dead time (HOPDT) process model.

⋆ This work was supported by a grant of the Romanian Ministry of Research, Innovation and Digitization, PNRR-III- C9-2022–I8, grant number 760068/23.05.2023 and by a grant of the Romanian Ministry of Education and Research, CNCS- UEFISCDI, PN-III-P1-1.1-PD-2021-0204.


10.1016/j.ifacol.2024.08.566

The paper is structured as follows. Section 2 details the design methodology and guidelines for a proper construction of the sinusoidal test input signal. Section 3 details the idea of using the impulse response and a generating filter to produce precise HOPDT estimation even in the presence of stochastic disturbances. Section 4 presents two numerical examples to validate the proposed approach. The last section includes final conclusions and further possible research directions.

## 2. DESIGN METHODOLOGY

The process transfer function $P(s)$ is assumed to be unknown.

**Step 1** Choose a test frequency $\bar{\omega}$, i.e. the process critical frequency $\omega_c$: $\angle P(j\omega_c) = -180^o$. The method works for any test frequency. However, a frequency near to (not exactly at) the critical frequency is the most interesting choice. At lower frequencies, the magnitude and phase do not change much, while at higher frequencies, the magnitude decreases fast and these frequencies thus become less-and-less important. An acceptable estimate of the critical frequency can be obtained by a preliminary relay test or step test.

**Step 2** Design a sinusoidal test input $u(t)$ with the frequency $\bar{\omega}$, further referred to as the IR (impulse response) - explorer signal. Details on the properties of $u(t)$ are given later on.

**Step 3** Apply the signal $u(t)$ to the process and measure the resulting output signal, $y(t)$. Notice in practice $y(t)$ may contain noise.

**Step 4** Calculate the IR-extractor:

$$h = \frac{\ddot{y}(t) + \bar{\omega}^2 y(t)}{\bar{\omega}} \tag{1}$$

and average to obtain the process impulse response $h(t)$. Details regarding (1) are given in Section 3. The result of this step is an estimate of the process IR h(t); it is perfect in absence of stochastic disturbances. The method is robust to disturbances as it will be shown Section 3.

**Step 5** Using the Discrete Fourier Transform (DFT) method, calculate the complex numbers $P_i = P(j\omega_i)$, where $\omega_i = 0.80\bar{\omega}, 0.85\bar{\omega}, ..., \bar{\omega}, ..., 1.15\bar{\omega}, 1.20\bar{\omega}$. The results in Section 3 show that in this range, stochastic disturbances are rejected, and the frequency response can be estimated with increased accuracy.

**Step 6** Use the 9 complex numbers $P_i$ from Step 5 to estimate a HOPDT transfer function.

### 2.1 The IR-explorer and IR-extractor properties

An example of the IR-explorer and IR-extractor signals is given in Fig. 1. The proposed test signal $u(t)$ contains 4 sections (indicated by the red arrows in Fig. 1, upper plot) as the result of the summation of 4 sine signals with frequency $\bar{\omega}$. The first one is a positive sine, from which the unit IR in $h(t)$ can be extracted (De Keyser et al. (2022)). The second signal is the negative sine delayed by the process settling time (ST). The third signal is the negative sine delayed twice ST with respect to the first sine signal. These will produce negative impulses. The fourth signal is the positive sine, but delayed by three times the ST. This will produce a positive impulse response. The summation of these 4 sine signals results in the test sequence IR-explorer signal. The duration of each section of the IR-explorer should be selected close to the process ST and contain an integer number of sine periods. The IR coefficients go to zero after this minimal signal length. The resulting four IRs are averaged to improve the SNR in case of stochastic disturbances affecting $y(t)$. In absence of noise, only the first section of the IR-explorer signal $u(t)$ is required. In most common applications, 2-4 sections are enough to produce a good estimation of the impulse response. For very noisy signals, to reduce the SNR, more sections of the IR-explorer signal $u(t)$ can be used.

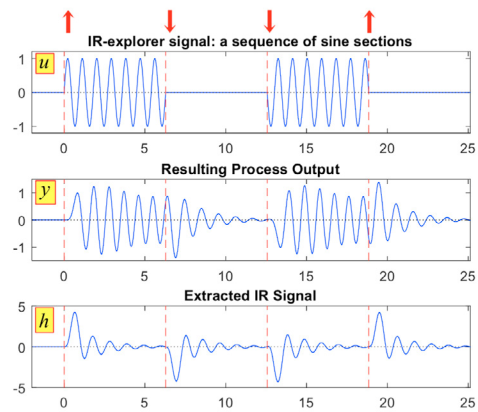


Fig. 1. The IR-explorer, resulting process output $y(t)$ and the resulting IR-extractor signals. Red arrows indicate the test signal sections

Once the IR $h(t)$ has been obtained, the classical frequency response is obtained:

$$P(j\omega) = \int_0^\infty h(t) e^{-j\omega t} dt \tag{2}$$

with Discrete Fourier Transform (DFT) at each frequency $\omega_i$,

$$P_i \cong T_s \sum_{k=0}^{N_s-1} h_k e^{-j\Omega_i k} \tag{3}$$

where $t = kT_s$, $T_s$ is the sampling period, $N_s$ is the number of measured samples, $h_k = h(kT_s)$ and $\Omega_i = \omega_i T_s$ is the constant discrete frequency.

**Remark**: **The method is suitable for stable processes. For integrating processes, closed loop tests are used instead to estimate the IR-extractor.**

For a known controller transfer function $C(s)$, the result of the closed loop test consists in the impulse response of the closed loop system $T(s)$, which is used to determine the frequency response points $T_i = T(j\omega_i)$. Then, the process frequency response points can be easily computed using $P_i = \frac{T_i}{C_i(1-T_i)}$.

### 2.2 Principle of HOPDT modeling

Given, the following HOPDT model having $N_a$ poles and $N_b$ zeros, with $N_a > N_b$:

$$M(s) = \frac{b_{N_b} s^{N_b} + ... + b_1 s + b_0}{a_{N_a} s^{N_a} + ... + a_1 s + 1} \exp^{-\tau s} \tag{4}$$

where $b_0$ is assumed to be fully known (i.e. it is the static gain) and $\tau$ the time delay, define a cost function:

$$V(\tau, \theta) = \sum_i |P(j\omega_i) - M(j\omega_i)|^2 \tag{5}$$

where $\theta = [a_1 a_2 ... a_{N_a} | b_1 b_2 ... b_{N_b}]$ and $0.8\bar{\omega} \leq \omega_i \leq 1.2\bar{\omega}$. The FR-points $P(j\omega_i)$ of the unknown process are estimated using the proposed method based on the IR-extractor signal and (3) for the same frequency points $\omega_i$. To estimate (4), the minimization of the cost function in (5) is performed using the standard Non Linear Least Squares (NLLS) algorithm with Gauss-Newton method:

$$\{\tau^*, \theta^*\} = arg \min_{\tau,\theta} V(\tau, \theta) \tag{6}$$

## 3. PRACTICAL IMPLEMENTATION TO DETERMINE IR

**Property**: deterministic test signals are the impulse response of a generating filter F(s).

A deterministic test signal is computed as: $U(s) = F(s)\Delta(s) = F(s)$, where $\Delta(s)$ is the Laplace transform of the Dirac impulse and thus $\Delta(s) = \mathscr{L}\{\delta(t)\} = 1$. The generating filter F(s) is thus simply the Laplace transform of the deterministic signal.

A sinusoidal test signal is proposed to be applied at the input of an unknown process, as indicated in Fig. 2. The resulting output signal is y(t). The principle of the method is presented in Fig. 3, where an estimate of the process impulse response $\hat{h}(t)$ is obtained. The idea is based on performing a swap between the process $P(s)$ and the filter $F(s)$ blocks.

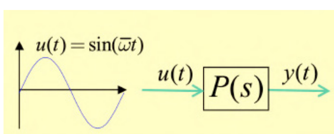


Fig. 2. The sinusoidal test signal applied at the input of an unknown process

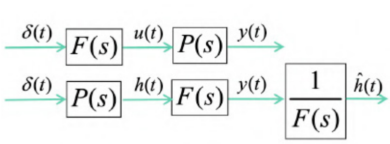


Fig. 3. Block diagram that produces the process impulse response

In this case, Y(s)=F(s)H(s), with the generating filter F(s) being:

$$F(s) = \frac{\bar{\omega}}{s^2 + \bar{\omega}^2} \tag{7}$$

Then, filtering the output signal y(t) with the filter $\frac{1}{F(s)}$, as indicated also in Fig. 3, produces the signal $\hat{h}(t)$ according to $\hat{H}(s) = \frac{1}{F(s)} Y(s)$. Quite frequently, in practical applications, the output signal $y(t)$ is affected by noise and disturbances. In this case, the output signal may be written as: $Y(s) = P(s)U(s) + D(s)$, where D(s) is the Laplace transform of the stochastic disturbance d(t), colored noise with zero mean value. In this case, the estimated impulse response $\hat{h}(t)$ is computed as:

$$\bar{H}(s) = \frac{1}{F(s)} Y(s) = \frac{1}{F(s)} [P(s)U(s) + D(s)] \tag{8}$$

Expanding the right hand side term in (8) and replacing $U(s) = F(s)\Delta(s) = F(s)$ leads to the following result:

$$\bar{H}(s) = \frac{1}{F(s)} P(s)F(s)\Delta(s) + \frac{1}{F(s)} D(s) = H(s) + \frac{1}{F(s)} D(s) \tag{9}$$

This last equation suggests that the estimated impulse response $\hat{h}(t)$ is the sum of the real impulse response $h(t)$ and the error signal $n(t)$, which includes all process output disturbances $d(t)$ filtered by the inverse of the generating filter $\frac{1}{F(s)}$. This result is indeed remarkable if one chooses the generating filter such as to block the disturbance $d(t)$ around the frequency of interest $\bar{\omega}$. This ensures an accurate estimation of the process frequency response point $P_i$ even in the presence of stochastic disturbances. In case of a sine test signal, as recommended in this paper, the resulting generating filter F(s) was indicated in (7). As a result, the inverse of this generating filter is defined as:

$$F^{-1}(s) = \frac{s^2 + \bar{\omega}^2}{\bar{\omega}} \tag{10}$$

and its magnitude is computed as $|F^{-1}(j\bar{\omega})| = 0$. Notice that this inverse sine filter blocks the disturbance in the frequency range $[0.8 - 1.2] * \bar{\omega}$. As a result, the frequency response values $P_i$ will be calculated accurately even in the presence of disturbances. A magnitude plot of the inverse generating filter in (10) is given in Fig. 4. Notice that each attempt to calculate frequency response values at other frequencies will successfully fail in the presence of noise. For comparison purposes, Fig. 4 also displays the inverse of the generating filter in the case of a unit step function, where $F(s) = \frac{1}{s}$ and thus $F^{-1}(s) = s$ with the magnitude $|F^{-1}(j\bar{\omega})| = \bar{\omega}$. In this case, the inverse of the generating filter will not block disturbances around the frequency of interest $\bar{\omega}$. Furthermore, it gives improved information for sine signal with frequencies as at Step 5 in Section 2.

**Remark**: In industrial control, it is common practice to use a lowpass filter on the measured process output y(t). In this approach, a 3rd order lowpass Butterworth filter is used, which is represented by a transfer function B(s) with no zeros and with 3 poles. The process output y(t) is in fact thus filtered by B(s)/F(s), which is a proper transfer function with 2 zeros and with 3 poles. At the same time the combination B(s)/F(s) cancels the high frequency amplification of 1/F(s) visible in Fig. 4. The cut-off frequency of B(s) is chosen 1 decade higher than the test frequency $\bar{\omega}$. As such, it has no effect on the estimation of $P(j\bar{\omega})$ nor on the estimation of frequency points in the range $[0.8 - 1.2] * \bar{\omega}$.

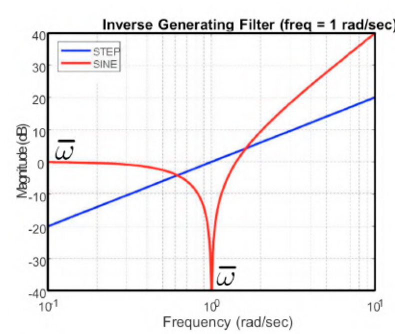


Fig. 4. Magnitude plot of the inverse generating filters corresponding to step and sine signals

## 4. NUMERICAL RESULTS

### 4.1 Example 1

The following process is considered here and assumed to be unknown:

$$P(s) = \frac{20}{(1 + 0.2s)^3 (s^2 + 1.2s + 36)} \tag{11}$$

with the critical frequency selected as the frequency of interest, $\bar{\omega} = \omega_c = 5.3$ rad/s and a settling time ST=7 seconds. A sine test input sequence is created with the frequency equal to $\omega_c$. The test input is indicated in Fig. 5, along with the measured output signal. Stochastic noise has been added. The real unit impulse response obtained using (11) is given in Fig. 5, along with the IR-extractor signal as obtained using the proposed approach.

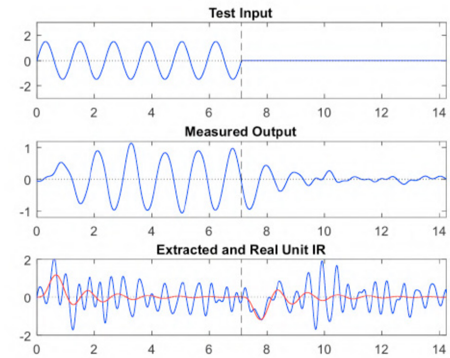


Fig. 5. Sine test to determine the process frequency response for example 1

The FR-points calculated using (3) for the frequencies as in Step 5 of Section 2 are indicated in Fig. 6, along with the Nyquist plot of the estimated HOPDT model, determined by solving the NLLS problem in (6):

$$HOPDT(s) = \frac{561}{s^4 + 15.63s^3 + 85.73s^2 + 554s + 1010} e^{-0.15s} \tag{12}$$

The results clearly support our claim that this method and data allow to accurately model the actual process frequency response using the HOPDT transfer function in (12).

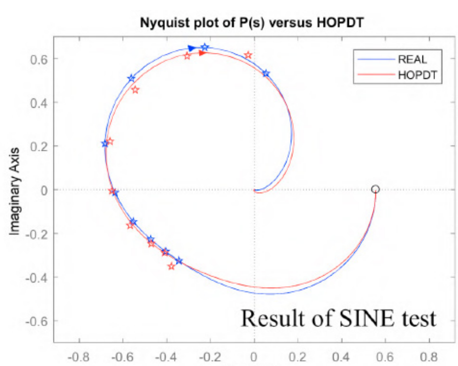


Fig. 6. Comparative frequency response plots of real process (obtained using (11)) and HOPDT model obtained using the proposed sine test method for example 1

Let us apply a unit step test with result in Fig. 7. The real IR from (11) and the extracted IR signal are given in Fig. 7, lower plot. Comparing against Fig. 5, lower plot, one might erroneously conclude that the step test will produce better estimations for the FR-points $P_i$. In fact, if one verifies the Nyquist plots as in Fig. 8, we demonstrate that the step test leads to inaccurate frequency response estimates. This is also expected from insight from Fig. 4.

To further validate the results, the Matlab 'tfest' function has also been used to estimate a higher order transfer function. The

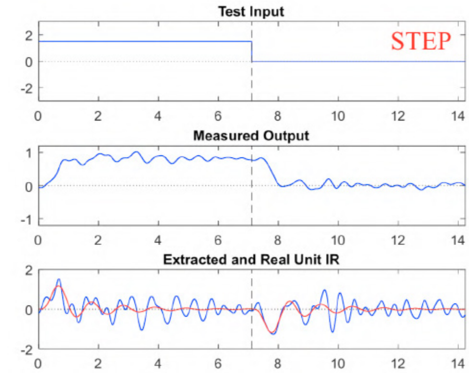


Fig. 7. Step test to determine the process frequency response points $P_i$ for example 1

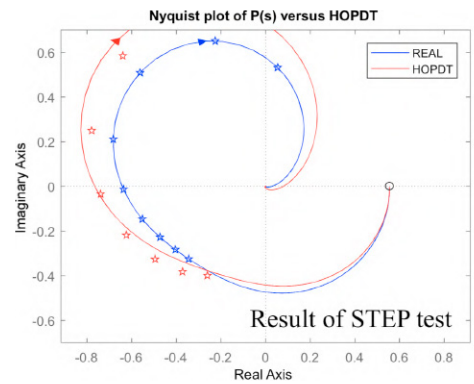


Fig. 8. Comparative frequency response plots of real process and HOPDT model obtained using the step response for example 1

step responses of the real process (11), of the HOPDT model in (12) and of the model estimated with Matlab (TFEST) are given in Fig. 9. This clearly shows that the proposed method, using the sine test, is efficient and accurate in estimating a HOPDT model.

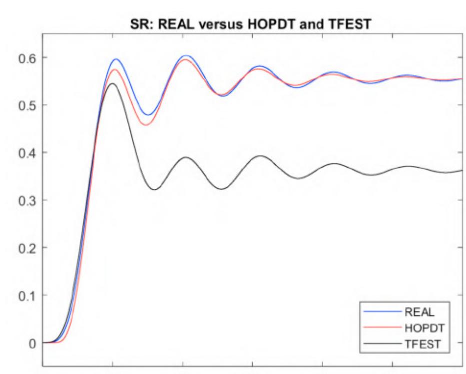


Fig. 9. Comparative step responses of real, HOPDT model and TFEST model for example 1

### 4.2 Example 2

The following third order process with large time delay is considered next:

$$P(s) = \frac{7}{(1+2s)(1+5s)(1+10s)} e^{-10s} \tag{13}$$

having the critical frequency $\omega_c = 0.135$ selected as the test frequency $\bar{\omega} = \omega_c$. To estimate the transfer function of the real unknown process in (13), stochastic disturbances on the input and output signals were considered. Two test sequences have been used, as indicated in Fig. 10 for a better signal-to-noise ratio. The estimation error signal is indicated in Fig. 11 for various orders of the $N_a$ and $N_b$ polynomials of the HOPDT model in (4). In this case, $N_a$=2 and $N_b$=0 was a compromise between minimum estimation error and complexity of the model.

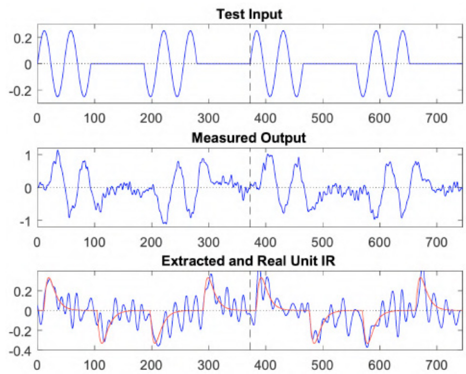


Fig. 10. Sine test data for example 2

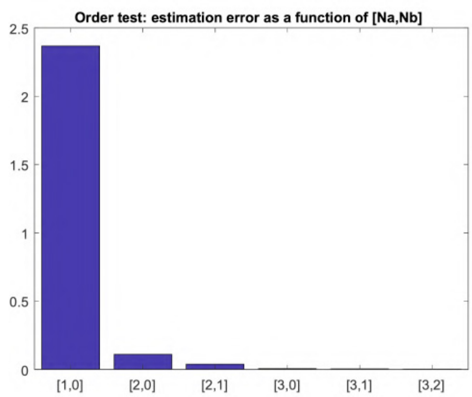


Fig. 11. Estimation error as a function of $[N_a, N_b]$ polynomials for example 2

Fig. 10 depicts the measured process output and the extracted and real impulse response. The extracted impulse response is further used to determine the FR-points $P_i$ using (3) for frequencies as in Step 5 giving:

$$HOPDT(s) = \frac{0.146}{(s^2 + 0.33s + 0.020)} e^{-12s} \tag{14}$$

The real process FR-values computed using the actual process in (13) as well as the process Nyquist plot are indicated in Fig. 12. The estimated FR-points and the Nyquist plot of the HOPDT model in (14) are indicated in the same figure. Yet again, an accurate estimation of the FR-values is possible using the proposed method, despite stochastic disturbances.

To further validate the results, the Matlab 'tfest' function has also been used to estimate a second order model. The step responses of the real process (13), of the HOPDT model in (14) and of the model estimated with Matlab (TFEST) are given in Fig. 13. This clearly shows that the proposed method, using the sine test, is efficient and accurate in estimating a HOPDT model.

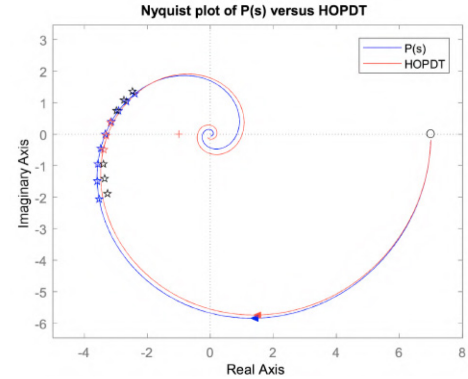


Fig. 12. Comparative frequency response plots of real process and HOPDT model obtained using the proposed sine test method for example 2

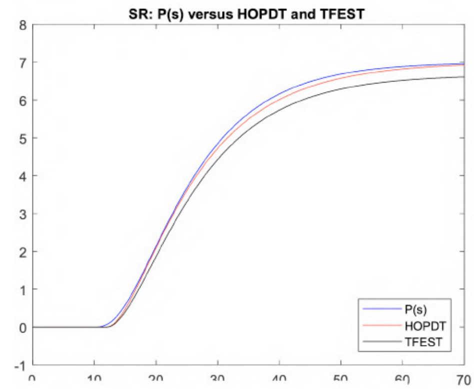


Fig. 13. Comparative step responses of real, HOPDT model obtained using the proposed method and TFEST model for example 2

To demonstrate the efficiency of the sine based method, in what follows a counterexample is presented where the step response is used in the estimation of a HOPDT model for the process in (13). Identical stochastic disturbances on both input and output signals have been used as in the previous case. The results of the step test, with the measured output, the extracted and real unit impulse responses are given in Fig. 14. The real FR-values computed for the frequencies in the range $\omega_i = 0.8\bar{\omega}, 0.85\bar{\omega}, ...., 1.15\bar{\omega}, 1.20\bar{\omega}$ using the process in (13), as well as the real Nyquist plot are given in Fig. 15. The FR-values $P_i$ computed for the same frequencies, but using (3), as well as the corresponding Nyquist plot of the resulting HOPDT model, are also indicated in Fig. 15. The Matlab 'tfest' function has also been used to estimate a model using the step test input from Fig. 14, upper plot. Fig. 16 shows the model estimation validation as a step response of the actual process in (13) and the HOPDT and TFEST models. Figures 15 and 16 clearly show that using a step test instead of the proposed sine test method leads to worse estimation of $P_i$ points and of the HOPDT transfer function. This is due to the disturbances affecting the signals, which are not blocked by the inverse generating filter, as it has been discussed in Section 3.

## 5. CONCLUSIONS

Quite frequently, in the industrial field, a process model is not available. Most of the times, this model is a poor estimate of the actual loop dynamics. A short sine test is used in this paper as

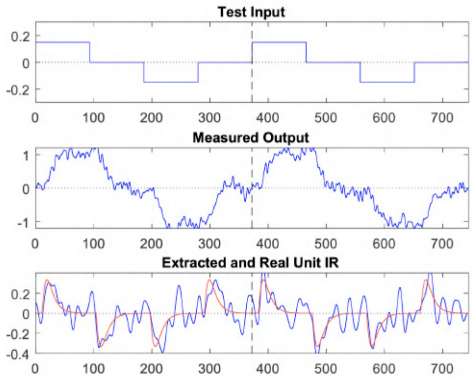


Fig. 14. Step test to determine the process frequency response points $P_i$ for example 2

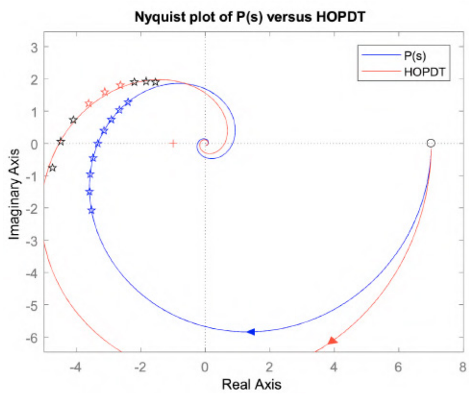


Fig. 15. Comparative frequency response plots of real process and HOPDT model obtained using the step response for example 2

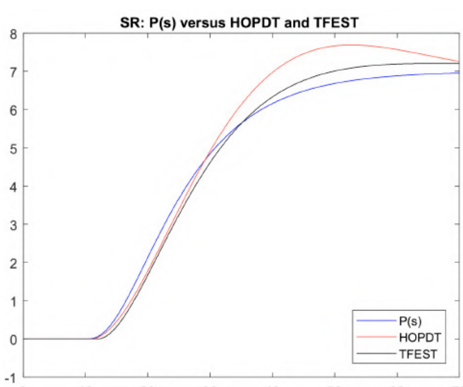


Fig. 16. Comparative step responses of real, HOPDT model and TFEST model for example 2

the basis to estimate the process impulse response. Although, greatly affected by stochastic disturbances, this impulse response allows to obtain good estimates of specific frequency response points. This remarkable result has been explained via theoretical insight in this paper. These frequency response points can be further used to estimate a transfer function model for the process. Numerical examples and comparisons are provided to demonstrate the efficiency of the proposed approach.

The high quality model obtained using the proposed method is more accurate than those obtained using classical step based identification methods. The method is reliable and less effort is required to produce very good process frequency response estimations. The advantages of the proposed method compared to other methods for transfer function estimation are threefold: 1) it requires a short duration test (highly important in industrial practice); 2) the test signal is a sine (which is better than a step and more easy to design than a multisine or PRBS) and 3) the sine test can be executed in open loop or in closed loop. Ongoing research applies this method on real industrial plants, as well as the comparison with existing methods of HOPTD estimation.

## REFERENCES

Albertos, P. (2014). Industrial process identification and control design: step-test and relay-experiment-based methods [book review]. *IEEE Control Systems Magazine*, 34(2), 78–80.

De Keyser, R., Birs, I.R., Copot, D., Ghita, M., Muresan, C.I., and Ionescu, C.M. (2022). Versatile solutions for the combine harvester header height control problem. In *2022 13th Asian Control Conference (ASCC)*, 221–226. doi: 10.23919/ASCC56756.2022.9828248.

De Keyser, R. and Muresan, C.I. (2019). Robust estimation of a sopdt model from highly corrupted step response data. *2019 18th European Control Conference*, 818–823. 25-28 June 2019, Naples, Italy.

Jianhong, W. and Ramirez-Mendoza, R.A. (2020). The practical analysis for closed-loop system identification. *Cogent Engineering*, 7(1), 1796895.

K.K. Tan, T.L. and Wang, Q. (1996). Enhanced automatic tuning procedure for process control of pi/pid controllers. *AIChE Journal*, 42(9), 2555–2562.

Liu, T., Wang, Q.G., and Huang, H.P. (2013). A tutorial review on process identification from step or relay feedback test. *Journal of Process Control*, 23(10), 1597–1623.

Ljung, L., Chen, T., and Mu, B. (2020). A shift in paradigm for system identification. *International Journal of Control*, 93, 173–180. doi:10.1080/00207179.2019.1578407.

Monje, C.A., Vinagre, B.M., Feliu, V., and Chen, Y. (2008). Tuning and auto-tuning of fractional order controllers for industry applications. *Control Engineering Practice*, 16(7), 798–812.

Muresan, C.I., Bunescu, I., Birs, R., and De Keyser, R. (2023). A novel toolbox for automatic design of fractional order pi controllers based on automatic system identification from step response data. *Mathematics, accepted*.

Xu, L., D.F. and Yang, E. (2020). Separable recursive gradient algorithm for dynamical systems based on the impulse response signals. *Int. J. Control Autom. Syst.*, 18, 3167–3177.

Xu, L. and Ding, F. (2017). Parameter estimation for control systems based on impulse responses. *Int. J. Control Autom. Syst.*, 15, 2451–2479.

Xu, L., Ding, F., and Zhu, Q. (2021). Decomposition strategy-based hierarchical least mean square algorithm for control systems from the impulse responses. *International Journal of Systems Science*, 52(9), 1806–1821.

Ziegler, J.G. and Nichols, N.B. (1942). Optimum Settings for Automatic Controllers. *Transactions of the ASME*, 64, 759–76. doi:10.1115/1.2899060.

Åström, K. and Hägglund, T. (1984). Automatic tuning of simple regulators with specifications on phase and amplitude margins. *Automatica*, 20(5), 645–651.

Åström, K. and Hägglund, T. (2004). Revisiting the ziegler–nichols step response method for pid control. *Journal of Process Control*, 14(6), 635–650.